We are IntechOpen, the world's leading publisher of Open Access books Built by scientists, for scientists

6,900
Open access books available

186,000
International authors and editors

200M
Downloads

Our authors are among the

154
Countries delivered to

TOP 1%
most cited scientists

12.2%
Contributors from top 500 universities

WEB OF SCIENCE™

Selection of our books indexed in the Book Citation Index in Web of Science™ Core Collection (BKCI)

Interested in publishing with us?
Contact book.department@intechopen.com

Numbers displayed above are based on latest data collected.
For more information visit www.intechopen.com

Chapter

Thick-Section Epoxy Composites

Yanan Hou, Liguo Li and Joseph H. Koo

Abstract

Thick-section composites (TSC) are extensively demanded in many fields, such as aerospace, wind energy, and oil and gas industries. However, the manufacturing process of thick-section thermoset composites (TSSC) encounters significant complexities, such as variations of nonuniform resin flow, exothermal reaction and curing, and dimensional stability through the thickness direction. These process-related nonuniformities are expected to result in through-thickness gradients of mechanical properties and curing-induced deformations, leading to undesirable residual stresses and damage. This chapter introduces the application of TSC and issues related to its manufacturing processes. Methods of TSC are examined and analyzed. Fundamental characteristics of curing kinetics, thermal transfer, and residual stress in TSC will be explained. Research of detailed experiments will be referred for readers for further studies.

Keywords: thick-section, thermoset, composite, glass fiber, carbon fiber, crack, micro-crack, manufacturing, residual stress, coefficient of thermal expansion, heat transfer, wrinkles, porosity, wind energy, wind turbine blade, oil and gas, downhole tools, curing kinetics, curing shrinkage, waste disposal, DSC, DEA

1. Introduction

To differentiate thin-section composites and composite film, fiber-reinforced composites (FRC) with cross-sections of 1 inch or thicker are generally known as TSC, regardless of the geometry of the part. Well-known of its low cost and high strength-to-weight ratio, TSC are widely used in aerospace, wind energy, oil and gas industries, and others. For examples, a 100-meter-long offshore wind turbine blade can be made of FRC with a cross-section as thick as 3 inches. A composite oil tool can require a thickness up to 2 inches. However, the manufacturing process of TSSC encounters significant complexities, such as variations of nonuniform resin flow, exothermal reaction and curing, and dimensional stability through the thickness direction. These process-related nonuniformities are expected to result in through-thickness gradients of mechanical properties and curing-induced deformations, leading to undesirable residual stresses and damage. This chapter introduces the application of TSC and issues related to its manufacturing processes. Methods of TSC will be examined and analyzed. Knowledge on the fundamental characteristics of curing kinetics, thermal transfer, and residual stress in TSC will be explained. This chapter focuses on method explanation. Researches of detailed experiments will be referred for readers to further studies.

2. Application of TSC

Due to its high strength-to-weight ratio, composite material is widely applied in aerospace industry, wind energy, oil and gas, automotive industry, sports, and construction and agricultural equipment. Some of the state-of-the-art applications include high-temperature composite material that developed to work in extreme environments up to 700°F continuously could be potentially used by engine original equipment manufacturers (OEMs). Carbon fiber/epoxy rebar is developed to replace steel for construction. Sprayer boom arms made of carbon fiber/epoxy could range from 100 to 150 ft. long for agricultural equipment. In aerospace industry, aircraft interiors are widely made of epoxy pre-preg material. In the world's largest commercial aircraft, A380, 16% of the structural weight is made of advanced polymer composites, where the carbon fiber composite center wing box weighs over 9 tons. Fuselage panels and stabilizers add another 4% composite by weight [1]. In oil and gas industry, composite, other than metal, is increasingly used in pipeline to lower its weight and increase its flexibility. Composite downhole tools are favored due to their ease of disposal. In sports, composite material is found in bike frames, kayak paddles, dog handles, and more. In wind energy, fiber-reinforced composites are utilized in wind turbine rotor blades. The traditional automotive industry is inertia to replace metal by composites, but the emerging electric vehicle market offers opportunities to composite manufacturing technologies, including carbon fiber/epoxy sheet molding compound (SMC) wheels, lift gates, and composite battery enclosures. Filament wound liquefied petroleum gas (LPG) tanks are used for industrial and home gas storage. Pultruded composites are used as ballistic panels to protect school.

Besides replacing metal and wood, composite could also be a potential substitute of natural rocks due to its long-lasting nature. For example, stone carving is believed to be the most reliable method to storage information, which is able to retain its data for thousands of years, compared with paper that could last for hundreds of years or hard drive for less than 20 years in well-maintained storage environments. Polymer composites, coupled with laser or water printing technologies, might be used as a media to record information and be stored under water, for example, in the sea. Researchers at Virginia Tech's College of Science are also working on porous carbon fiber made from block copolymers, similar to a sponge, to store ions of energy [2].

As the world population reached 7.6 billion and expected to almost double in the next hundred years, many composite equipment are required to become larger and thicker. For example, the global offshore wind energy market grew by 0.5% in 2019, with new installations of 4.49 gigawatts [3]. A common seen wind turbine in the USA is Gamesa G87 made in Spain with turbine blades of 43.5 meter long. Its capacity is 2 megawatts. Wind turbines of increasingly larger capacities are demanded. A prototype 100-meter-long offshore wind turbine blade made of FRC has a cross-section up to 3 inches thick. Another example is in aerospace; Northrop Grumman is adapting its automated stiffener forming technology to build spars. Thickness of most stiffeners is less than 0.25 inch, but that of spars can be 1 inch or thicker [4], which will dramatically increase the complexity of the manufacturing process.

3. Thick-section epoxy composite (TSEC)-related issues

3.1 Micro-cracks

Comparing to thin-section composites, the manufacturing of TSEC introduces superimposed complexities. Micro-cracks are often found in TSC, which largely

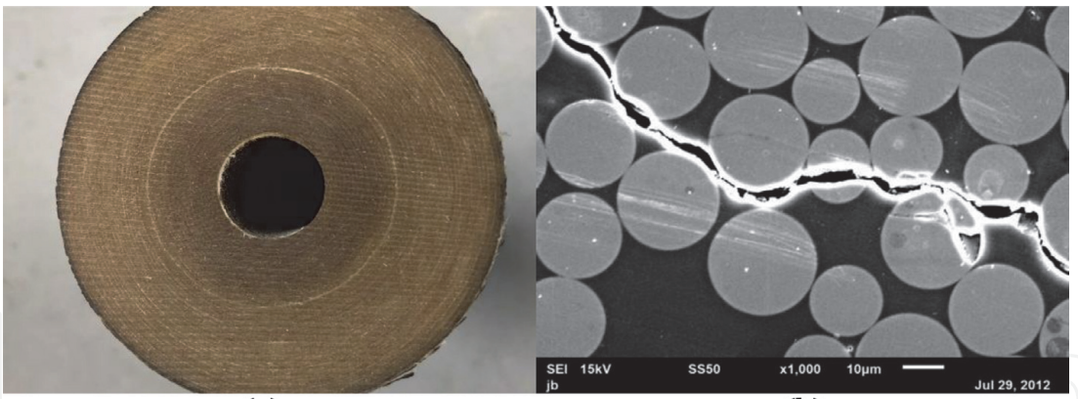

Figure 1.
TSC with micro-cracks. (a) TSC with micro-cracks. (b) Micro-cracks under SEM.

deteriorate the consistency of its mechanical properties. Micro-cracks can be visually examined as shown in **Figure 1(a)**. A graph of micro-crack under scanning electron microscopy (SEM) is shown in **Figure 1(b)**.

Micro-cracks are mainly caused by the internal stress generated during the curing of the composites and the cooling process. The internal stress of TSEC is affected by the following parameters.

3.1.1 Curing shrinkage

Epoxy is a thermoset polymer generally superior to polyester and vinyl ester in terms of mechanical properties and cost. Epoxy resin can be thermally cured or cured with a wide range of hardeners at room temperature or elevated temperatures, including amine, anhydrides, phenols, alcohols, and thiols. Cross-link reactions of epoxy accompany with curing shrinkages. The shrinking is a continuous process along with the increase of the degree of curing of the material. For example, a standard bisphenol A epoxy (e.g., Epon 828) shrinks 2.8% pre-gelation and 2.5% post-gelation [5]. Curing shrinkage of epoxy can be up to 9%.

3.1.2 Nonuniformity of heat distribution

Curing speed of epoxy is positively related to temperature. Meanwhile, the cross-linking reaction releases heat, which adds an additional item to the already complex heat transfer equation. The main author's earlier research [6] shows the temperature difference of a 3.6-inch-thick FRC can be up to 52°C in the thickness direction, with the hottest layers in the middle of the part. The temperature gradient leads to a curing degree difference of up to 70% in the thickness direction. This implies when the epoxy resin in the middle of the part is solidified, epoxy resin at outer surfaces is still in liquid state. While the epoxy resin at the outer surfaces is solidified, the accompanying volume shrinkage generates stress among the surface layers and the already solidified middle layers. The residual stress can be high enough to create micro-cracks among layers. Complexities piles up when dealing with epoxy systems requiring elevated temperature curing cycle. For example, a filament wound TSC billet may take 4 hours to wind, resin in layers closer to inside diameter (ID) cures hours earlier than the outer layers. Once the billet is moved into an oven after winding for further curing, it may take a couple of hours for the heat transferring to the core. Outer layers cure faster than the inner layers at the beginning, and the middle layers come from behind later due to heat overshoot caused by

the reaction. As a result, micro-cracks often occur between middle layers and the ID or between middle layers and the surface, as shown in **Figure 1**.

3.1.3 Coefficient of thermal expansion (CTE)

Thermal expansion coefficient of epoxy is over 10 times higher than that of glass or carbon fibers that are widely applied as reinforcement in FRC. A curing profile of FRC usually includes several steps of heat soaking and cooling down, during which, bonds between the resin and its reinforcement face repeated stress and fatigue, where failure leads to interlaminar cracks. Tooling complexes the problem with an additional thermal expansion coefficient in resin transfer molding (RTM) or filament winding (FW) processes.

3.2 Mechanical property nonuniformity

Unlike most metallic materials with isotropic properties, FRCs often exhibit anisotropy properties. For example, a glass fiber-reinforced TSC laminate displaces various mechanical properties in different directions. As shown in **Figure 2**, tensile strength in the fiber direction (LZ direction) is over 30 times higher than that in the thickness direction (ZT direction) [7].

Tensile strength of glass fibers (e.g., 321–343 Ksi for a commercial E glass fiber) is over 34 times higher than that of the matrix epoxy (e.g., 9.7 Ksi for a bisphenol A epoxy), and the Young's modulus of glass fibers (12.1×10^6 psi for a commercial E glass fiber) is over 25 times higher than that of the matrix epoxy (0.45×10^6 psi for a cycloaliphatic epoxy cured with an anhydride curing agent). Mechanical properties of FRC along fiber directions are dominated by properties of fibers; those that are transverse to fibers are weakened by resin matrix and bonds between epoxy and fibers.

Mechanical properties of epoxy are determined by its cross-linking density, which is controlled by its curing profile. For example, a rapid cure may result in a quick but sloppy cross-linking, and a low curing temperature may leave the epoxy not fully cured. In theory, a slow curing process with a rationally higher maximum curing temperature is always preferred, but it can be costly and infeasible in a production scale.

Glass transition temperatures (T_g) are often used to imply mechanical properties of post-gelled epoxy. T_g represents the temperature where epoxy transits the fastest

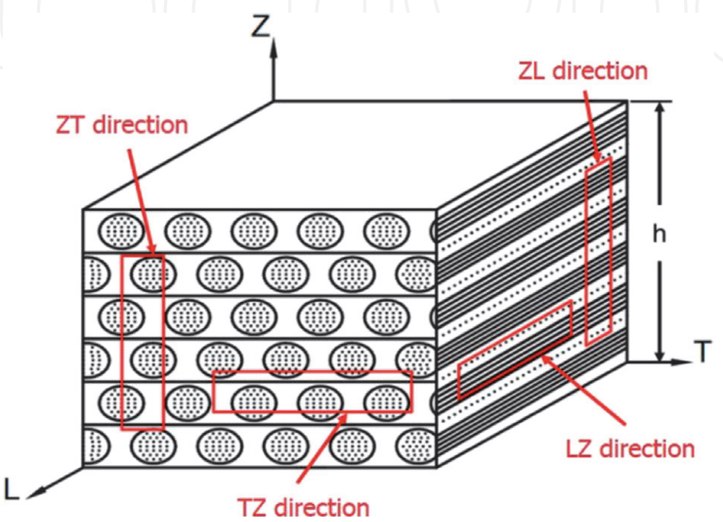

Figure 2.
Schematic diagram of continuous fiber-reinforced TSC.

from "glassy" state to rubbery state. The main author's earlier research [6] shows the T_g difference of a 3.6 inch TSC laminate can be up to 15°F. T_g differences are caused by temperature gradients in the TSC part during the curing process, and the variation of mechanical properties lowers the quality of the composite part.

3.3 Wrinkles and porosities

Epoxy, with trapped air, flows among fibers before gelation, causing relaxation of fibers and dry spots. This often results in wrinkles and porosities, especially in TSCs. Wrinkles and porosities dramatically deteriorate matrix-dominated properties and can severely limit the performance of the TSC parts. Researches show lower curing pressure reduces wrinkles but may increase porosities [8]. Correct design of process parameters and accurate measurements are essential to quantify and eliminate manufacturing defects. For example, in FW, a gap between feeding fiber bands creates fiber waviness and results in pineapple-like skin, as shown in **Figure 3**.

Porosity is a major concern of TSC manufacturing, especially of pre-preg/tow-preg processed TSC. Fibers pre-coated with resin are laid up to required thickness and shape before curing. During the curing process, coating resin is liquefied, filled in gaps between fibers, and then solidified. Trapped air among fibers requires time to escape before the gelation of resin. Thus, TSC made with pre-preg/tow-preg process often yields relatively higher porosity. **Figure 4** shows the void under SEM.

Figure 3.
TSC with pineapple-like skin.

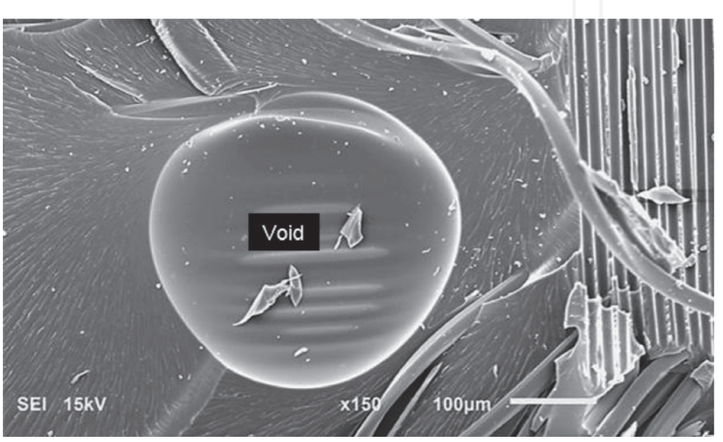

Figure 4.
Void in TSC under SEM.

3.4 Waste disposal and heat overshoot

Gelation happens after either mixing resin and hardener or adding catalyst into homopolymerizing resin. Excess mixed epoxy or epoxy squeezed out during processing is hard to recycle and turns out to be waste. Even with an effective waste reducing plan, the quantity of production epoxy waste from TSC manufacturing is often considerable. Disposing the waste under the Resource Conservation and Recovery Act (RCRA) rules can be costly and complicated. The waste can be categorized into three scenarios [9]:

- Disposal resin, hardener, or catalyst before mixing. It's often ignitable hazardous waste (EPA waste code D001) or corrosive waste (EPA waste code D002). A waste company specialized in chemical disposal is required to handle the waste, which can cost around $25 per gallon, plus transportation and fuel.

- Disposal mixed resin that is not fully cured. It may be subject to both solid waste (40 CFR 261.3) and unused commercial chemical product (40 CFR 261.33). It may be on the P and U lists of chemical product waste, and none of the F or K lists for specific and non-specific sources of hazardous waste will apply.

- Disposal fully cured epoxy. This scenario is the easiest to deal with. Fully cured epoxy rarely exhibits hazardous waste characteristic and can be disposed as general solid waste.

In the industry, pure resin/hardener or unfully cured waste is usually stoichiometrically mixed with hardener/resin and fully cured before disposal. A waste disposal curing profile should be carefully designed to avoid reaction overheat and burning accidents.

4. Methodologies of TSEC analysis

4.1 Curing kinetics characterization

Differential scanning calorimeter (DSC) is often used to characterize the kinetics of thermoset resins. Data can be used to study the relationship between curing degrees and temperature. Kamal-Sourour relationship is usually used in the curing kinetics study of pure bisphenol A epoxy, as shown in Eq. (1).

$$\frac{da}{dt} = ka^m(1-a)^n \tag{1}$$

where a is the degree of cure, T is the instantaneous temperature, m and n are orders of the reaction, and k is the rate of constant, following the Arrhenius relationship.

$$k = Aexp\left(-\frac{\Delta E}{RT}\right) \tag{2}$$

The ΔE in Eq. (2) is the activation energy of the epoxy, A is the frequency factor, and R is the universal gas constant. To obtain the material parameters, three DSC

isothermal tests are usually conducted. The three temperatures can be selected in the following way:

1. Conduct a temperature scanning on the epoxy of interest at 5°C/min using DSC.

2. Select the reaction initiation temperature as the first temperature, which is implied by the start of an uptrend of the heat flux curve. Isothermal test at this temperature captures cure kinetics characterization of the beginning of the curing reaction.

3. Select the second temperature by drawing tangential lines, one along the heat flux curve before reaction starts and one at the fastest reacting point before the first peak.

4. Select a temperature a little lower than the first peak temperature as the last temperature. Isothermal test at this temperature starts fast. It tends to lose track on some heat at the beginning of the reaction, but captures characterization of the cure kinetics at the latter part of the reaction.

For example, **Figure 5** shows heat flux of a commercial resin from a DSC temperature scanning at 5°C/min. The three temperatures for isothermal tests can be 22, 50, and 70°C.

Degree of cure and curing rate can be calculated from DSC data, and three curves of curing rate versus degree of cure can be plotted at each test temperature (T1, T2, and T3). The reaction orders and the rate of constant in the reaction kinetics model can be determined by a nonlinear fitting method using either curing kinetics software or MATLAB. The activation energy (ΔE) and lnA can be obtained by a linear fitting of lnk and $1/T$.

Bailleul's [10] equation is often used for more complex polymerization reactions, as shown in Eq. (3).

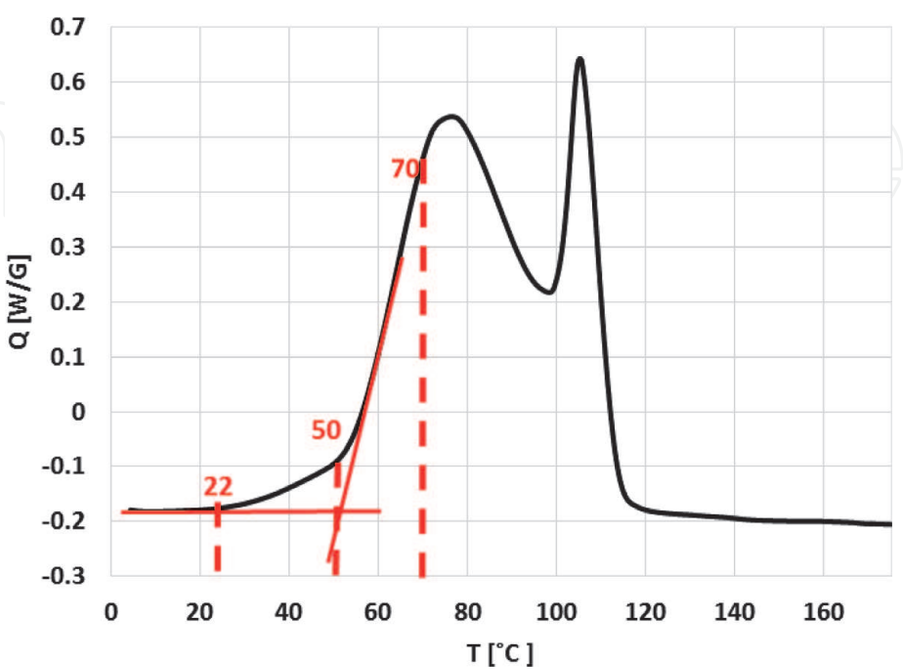

Figure 5.
DSC experiment for isothermal temperature selection.

$$\frac{da}{dt} = W(v(T)) \cdot K(T) \cdot G(a) \cdot F_{diffusion}(a) \tag{3}$$

where $W(\nu(T))$ represents the induction of reaction or the inhibition period when an inhibitor is added to the resin. It defines as below:

$$W\left(v(T) = \begin{cases} 0, if\ v(T) \geq 0 \\ 1, if\ v(T) < 0 \end{cases}\right. \tag{4}$$

$v(T)$ is expressed as Eq. (5).

$$v(T) = t_{ref} - \int_0^{t_{ind}} exp\left[-B \cdot \left(\frac{T_{ref}}{T} - 1\right)\right] dt \tag{5}$$

$K(T)$ represents the dependence of curing rate on temperature, as shown in Eq. (6), $G(a)$ represents the dependence of curing rate on the degree of cure as shown in Eq. (7), and $F_{diffusion}(a)$ describes the diffusion control in the curing, as shown in Eq. (8).

$$K(T) = K_{ref}\, exp\left[-A\left(\frac{T_{ref}}{T} - 1\right)\right] \tag{6}$$

$$G(a) = \sum_{i=0}^{6} G_i a^i \tag{7}$$

$$F_{diffusion}(a) = \frac{1}{1 + exp\,(E_1(a - a_c))} \tag{8}$$

The equation fits well in the reaction of DERAKANE MOMENTUM 411–350 epoxy vinyl ester and 1 wt% NOROX MEKP-925H (MEKP stands for methylethylketone peroxide) with 0.05 wt% of cobalt naphthenate well [11].

In situ degree of curing can be quantified by dielectric cure analyzer (DEA). DEA sensors can be embedded during the manufacturing process of TSC and measures in situ ion viscosities (ρ) of the matrix resin. Resin ion viscosity is positively correlated with its degree of cure and negatively correlated with temperature. Curing index, which is equivalent to degree of curing, is calculated as Eq. (9).

$$CI = \frac{log\left[\sigma_{f_0}(a, T_0)\right] - log\left[\sigma_{f_0}(0, T_0)\right]}{log\left[\sigma_{f_0}(1, T_0)\right] - log\left[\sigma_{f_0}(0, T_0)\right]} \times 100\% \tag{9}$$

where σ is the ion conductivity of the material, which is the reverse of ion viscosity. The subscript f represents the frequency of the voltage of excitation used in the DEA test. The temperature and frequency with the subscript 0 refer to the testing frequency and temperature of the curing index calculation. The main author's previous study [12] showed well agreement of curing index and degree of cure in AOC Altek R920-E polyester mixed with a 2% NOROX MEKP-925 catalyst and glass fiber-reinforced composites.

In TSC analysis, thermocouples are usually placed at locations of interest to record the temperature history during manufacturing processes, including pre-curing process, curing process, and post-curing process. Curing degree profiles at various locations are calculated by inputting temperature history into the predetermined curing kinetics model. In situ curing index profiles can be measured

using DEA sensor and related to degrees of cure. The degree of cure profiles can be used to optimize the curing profile of the composites and evaluate properties of the end composite part. For example, the glass transition temperature can be modeled through a function of degree of cure developed by Pascault et al. [13], as shown in Eq. (10).

$$\frac{T_g - T_{g0}}{T_{g\infty} - T_{g0}} = \frac{a \cdot k}{1 - (1 - k) \cdot a} \tag{10}$$

where T_{g0} is the glass transition temperature of raw epoxy and $T_{g\infty}$ is the glass transition temperature of fully cured epoxy. k is a structure-dependent parameter that can be obtained by nonlinear fitting of T_g and curing degree data from DSC tests.

Curing degree profiles also provide essential parameters for further curing shrinkage and inner stress study.

4.2 Heat transfer characterization

Heat transfer of thermoset composite differentiates itself from metal materials primarily on three aspects: (1) changing specific heat capacity, (2) changing thermal conductivity coefficient, and (3) reaction heat.

4.2.1 Specific heat capacity

Specific heat capacities of composite are usually calculated using mixing law as shown in Eq. (11).

$$C_{p-composite} = C_{p-fiber} \cdot w_f\% + C_{p-epoxy} \cdot \left(1 - w_f\%\right) \tag{11}$$

where w_f % represents the weight percentage of reinforced fiber.

Specific heat capacities of epoxy depend on temperature and degree of cure, where a mix law may also be established, as shown in Eq. (12).

$$C_{p-epoxy}(T, a) = C_{p0}(T) \cdot a + C_{p1}(T) \cdot (1 - a) \tag{12}$$

where C_{p0} is the specific heat capacity of raw epoxy, C_{p1} is the specific heat capacity of fully cured resin, and a is the degree of cure.

Modulated DSC tests are usually used to capture reversible heat flux of thermoset resin, which can be used to calculate the specific heat, as shown in Eq. (13).

$$C_p(T) = \frac{-q}{m \cdot dT/dt} \tag{13}$$

where q represents heat absorbed by the material to increase one-unit degree of temperature, m represents the mass of the material, and T represents the temperature. For unreacted epoxy, DSC scanning includes several plateaus at temperatures below the reaction initiating temperature. Three heating speeds are normally applied. 5°C/min, 10°C/min, and 20°C/min are normally selected. A curve fitting of specific heat capacity versus temperature yields the relationship between specific heat capacity of unreacted resin and temperature. The relationship between specific heat capacity of fully cured resin and temperature can be obtained through similar DSC scanning with plateaus including several temperatures higher than the glass transition temperature of the material and several temperatures lower. For

example, Bailleul et al. [14] selected 30, 70, and 100°C for the raw material and 30, 70, 110, 150, and 190°C for the fully cured resin, where the initiation temperature of the resin is higher than 100°C and the T_g of the fully cured resin is about 130°C. In Bailleul et al.'s research, curve fittings present linear relations between the heat specific capacity and temperature for all three scenarios: raw resin, cured resin before the glass transition period, and cured resin after the glass transition period. For fully cured resin during the glass transition, the specific capacity can be modeled using the value of C_p in the glassy state and C_p in the rubbery state, as shown in Eq. (14).

$$C_{p-glass\ transition}(T) = C_{p-glass}(T) \cdot (1 - \mu(T)) + \mu(T) \cdot C_{p-rubbery}(T) \tag{14}$$

$\mu(T)$ is expressed by Eq. (15).

$$\mu(T) = \frac{1}{2}\left(1 + tanh\ \left(\frac{d}{c} \cdot T + e\right)\right) \tag{15}$$

where d is the temperature range of the glass transition period. c and e can be determined through cure fittings of the experimental data.

4.2.2 Thermal conductivity coefficient

Like the specific heat capacity, thermal conductivity coefficients of composites along fiber direction can be calculated with the mixing law. Thermal conductivity coefficients of composites in the crosswise fiber direction can be calculated using a composite law with Springer-Tsai model, as shown in Eq. (16).

$$K_{composite} = K_{epoxy} \cdot \frac{\left(1 + v_f\%\right) \cdot K_{fiber} + \left(1 - v_f\%\right) \cdot K_{epoxy}}{\left(1 + v_f\%\right) \cdot K_{fiber} + \left(1 + v_f\%\right) \cdot K_{epoxy}} \tag{16}$$

where $v_f\%$ represents the volume fraction of fiber. Values of solidified composite parts can be verified by thermal conductivity meters, such as the TA instrument LaserComp Fox314.

Thermal conductivity of epoxy also depends on temperature and degree of curing, especially unfully cured epoxy. For example, Bailleul et al. [14] found the thermal conductivity of raw material increased proportionally over temperature, while fully cured resin varied small over temperature.

Thermal conductivity of unfully cured epoxy can be measured by TA instrument DXF 500/900 models. Like specific heat capacity testing profiles, raw epoxy should be tested at several temperatures below its reaction initiation temperature, and fully cured epoxy are tested at temperatures below and above the T_g.

For thermal conductivity tests on solid material, guarded hot plate method is usually applied. Heat is applied on the top or bottom surface of a sample, and temperatures on both of the top and bottom surfaces are measured to calculate the thermal conductivity coefficient by Eq. (17).

$$K = \frac{qL}{T_H - T_L} \tag{17}$$

where q is the quantity of heat passing through a unit area of the sample in a unit time, with the unit of [W/m^2], L is the distance between the top and bottom surfaces of the sample with the unit of [m], T_H represents the temperature of the warmer surface with the unit of [K], and T_L represents the temperature of the

cooler surface with the same unit. This method guarantees an accuracy of 98%, but it limits to low conductivity material, and it requires long measurement time and large specimen size [15]. It's often used to verify simulation values of solid FRC.

For liquid resin, hot wire or laser flash methods are usually applied. In a hot wire test, a heated wire is inserted into the material. Heat that flows out and temperature change in the wire are recorded to calculate the thermal conductivity. It's fast and with an accuracy up to 99% [15]. Laser flash method shoots short pulse of heat to the top surface of the sample, and temperature change is observed by an infrared scanner. This method requires small samples. It's fast and accurate at high temperatures but the instrument is expensive [15].

4.2.3 Resin enthalpy

The element that complexed the heat transfer calculation of thermoset composite is the reaction heat of unfully cured resin. The overall reaction enthalpy can be determined through a temperature scanning DSC test by integrating the heat flux over temperature. Enthalpy of epoxies that create different bonds during curing can vary dramatically. For example, a pre-catalyzed nadic methyl anhydride yields an enthalpy around 270 J/g in the reaction with a cycloaliphatic epoxy resin, while a formulated amine hardener yields a enthalpy around 410 J/g when reacted with a multifunctional epoxy resin.

Instantaneous reaction heat of an epoxy depends on degree of cure, curing rate, temperature, and fiber volume fraction. It can be represented by Eq. (18).

$$\dot{Q}_{reaction} = \frac{da}{dt}\left(1 - v_f\%\right) \cdot \rho_{resin} \cdot H_{enthalpy} \tag{18}$$

where a represents the degree of cure, $v_f\%$ is the fiber volume fraction, $H_{enthalpy}$ is the enthalpy of the epoxy, and ρ_{resin} is the density of the epoxy.

Like the density of water changes as it transfers to icy state, it's easy to imagine that the density of epoxy changes during its curing process, transferring from liquid to gelation and from glassy state to rubbery state. However, in the modeling of epoxy FRC, a constant epoxy density is usually applied, because (1) the existing of reinforcements lessened the flexibility of the volume change of epoxy and (2) the density change of epoxy is small. For example, the density change of MY750 epoxy is around 1% from unreacted state to fully cured state [16]. A density of 1.2 g/cm^3 is usually applied for epoxy. The density of composites can be calculated through the mix law.

With above illustrated parameters measured, the overall heat transfer governing equation can be used to model temperature histories of TSC at every locations of interest, as shown in Eq. (19). Thus, heat overshoot temperatures and locations can be predicted with the established model.

$$\begin{aligned}\frac{\partial}{\partial t}\left(\rho_{composite} C_{p-composite} T\right) = &\frac{\partial}{\partial x}\left(K_{xx-composite}\frac{\partial T}{\partial x}\right) + \frac{\partial}{\partial y}\left(K_{yy-composite}\frac{\partial T}{\partial y}\right) \\ &+ \frac{\partial}{\partial z}\left(K_{zz-composite}\frac{\partial T}{\partial z}\right) + \dot{Q}_{reaction}\end{aligned} \tag{19}$$

4.3 Residual stress characterization

Residual stress is introduced in epoxy TSC due to the curing shrinkage of epoxy and the mismatch between thermal expansion coefficient of the resin and reinforcements. Residual stresses, especially of TSC, are unevenly distributed in the

composites. This is caused by the mismatch between composite layers and temperature/curing gradients.

Curing shrinkage of composites can be calculated by Eq. (20) [11], where H is a hindrance factor and can be found experimentally.

$$CS_{composite} = CS_{resin} - v_f\% \cdot H \tag{20}$$

Curing shrinkage of unreinforced epoxy can be tested by rheology method [17, 18] or gravimetric method [16, 18]. Rheometers are usually used in the rheology method. Two heated parallel plates are used to measure the linear shrinkage of the resin, which can be transferred into volume shrinkage, with assumptions that resin is incompressible and zero in-plane strains. Resin shrinkage before gelation cannot be measured with this method. The gravimetric method is based on the Archimedean principle, with which, density of an object can be measured by immersed in a fluid. This method involves immersing a silicon rubber bag with the testing resin in a known fluid and measuring the density of the resin while curing it. This method is able to obtain the curing shrinkage information both before and after resin gelation. A linear relationship was found between the curing shrinkage and degree of cure by Shah and Schubel [17] using the rheology method and Khoun and Hubert [18] found a bilinear relation in their study using the gravimetric method, where the rate changed at gelation.

The CTE of composite can be obtained through micromechanics model, shown in Eq. (21) for the fiber direction and Eq. (22) for transverse and thickness directions.

$$a_1 = \frac{a_{1f}E_{1f}v_f\% + a_{1r}E_{1r}\left(1 - v_f\%\right)}{E_{1f}v_f\% + E_{1r}\left(1 - v_f\%\right)} \tag{21}$$

$$a_2 = a_3 = \left(a_{2f} + v_{12f}a_{1f}\right)v_f\% + \left(a_{2r} + v_{12r}a_{1r}\right)\left(1 - v_f\%\right) - \left[v_{12f}v_{f\%} + v_{12r}\left(1 - v_f\%\right)\right]a_1 \tag{22}$$

where the subscript f represents reinforcements, while r represents resin. The subscript 1 represents the fiber direction (longitudinal) and 2 represents the transverse direction. E is tensile modulus and v_{12} is Poisson's ratio.

Young's modulus and Poisson's ratio can be measured using stain gage and Instron machine at various temperatures [9]. White and Hahn [19] found that both have a linear relationship to the degree of cure at a constant temperature. In their study, it showed that the CTE remained relatively constant in the transverse direction and its change in the longitudinal direction was negligible compared to the effect of curing shrinkage. Thus, in many studies, constant CTEs are applied for the resin and reinforcements [20].

5. Recommendations

In TSC manufacturing industry, micro-crack issue is the first and foremost important. Micro-cracks dramatically decrease the uniformity of mechanical properties of the TSC parts, especially shear strengths along composite plies. One way to predict micro-cracks is to analyze the TSC manufacturing process in two scenarios: (1) treating it as a flow issue as the boundaries gel but the core flows and (2) treating it as a stress issue when no resin flows in the TSC part. For example, a 6-inch-thick 12 inch by 12 inch epoxy TSC part is manufactured by Vacuum Resin Infusion Process. The epoxy gels 1 hour after mixing resin and hardener at room

temperature. It takes 30 min to fully fill the entire part. After infusion, the part is placed in a convection oven for cure with a pre-subscribed temperature profile.

Due to the conventional heat inside the oven, resin at the outer surfaces of the part may solidify before the core curing to solid. In this scenario, the volume of the part is fixed by the solidified boundaries. Curing shrinkage of the core is the major cause of internal stress. The simulation can be simplified by separating the part into boundary (parts with gelled resin) and core (parts with ungelled resin). Gelation can be represented by degree of cure, which can be either simulated or tested by DEA. The shrinkage volume of the core after gelation can be simulated and compared to the current volume of the core. The total resin weight using to simulate the shrinkage volume of the core after gelation should be the total volume of resin infused into the part minus resin in the boundaries. A smaller shrinkage volume tends to result in micro-cracks at locations between layers in the core. This scenario is usually improved through the following methods:

- Infusing excess resin in the part through proprietary methods.

- Changing the solidification pattern of the part, e.g., B-stage the part before heating it up, or cool top surface, and/or heat bottom surface. For filament wound TSC billets, heating from inside out can largely reduce the chance of micro-cracks.

In the second scenario, after the part has no resin flowing, stresses develop between resin and reinforcements as well as among composite plies, due to degree of cure gradients. In the main author's earlier research [6], there was a 25% difference on degree of cure between the bottom and middle of the part. Internal stress in TSC parts at critical temperatures and degree of cures can be modeled and compared to the instantaneous strength of the composite. Larger stress predicts a high chance of micro-cracks. This scenario can be improved by adjusting curing profiles to avoid severe internal stress being built. B-stage and slower heating/cooling rate is usually helpful.

Acknowledgements

The support and motivation from Yanan and Liguo's family, their mom/mother-in-law, Shengmin Zhang, and their children, Leo Li and Landon Li, are greatly appreciated while Yanan and Liguo are writing this book chapter.

IntechOpen

IntechOpen

Author details

Yanan Hou[1*], Liguo Li[1] and Joseph H. Koo[2]

1 The WellBoss Company LLC, Houston, TX, USA

2 Department of Mechanical Engineering, The University of Texas at Austin, Austin, TX, USA

*Address all correspondence to: yanan.hou@thewellboss.com

IntechOpen

© 2020 The Author(s). Licensee IntechOpen. This chapter is distributed under the terms of the Creative Commons Attribution License (http://creativecommons.org/licenses/by/3.0), which permits unrestricted use, distribution, and reproduction in any medium, provided the original work is properly cited. CC BY

References

[1] Brosius D. An ode to the A380. Composites World. 2019;**5**:6

[2] Virginia Tech. Chemistry Researchers Use Block Copolymers to Create First Carbon Fibers with Uniform Porous Structure [Internet]. Available from: https://vtnews.vt.edu/articles/2019/02/mii-using-block-copolymers-to-make-porous-carbon-fibers.html#:~:targetText=Using%20block%20copolymers%20to%20create%20porous%20carbon%20fibers,-Liu%20used%20a&targetText=PAN%20is%20well%2Dknown%20in,removed%20to%20create%20the%20pores. [Accessed: December 11, 2019]

[3] CompositesWorld. GWEC Reports 51.3 GW of New Wind Capacity in 2018 [Internet]. Available from: https://www.compositesworld.com/news/gwec-reports-513-gw-of-new-wind-capacity-in-2018. [Accessed: December 11, 2019]

[4] Mason K. Spar forming simplified. Composites World. 2019;**5**:30-35

[5] Spencer JB. Cure Shrinkage in Casting Resins. United States: N.P.; 2015. DOI: 10.2172/1170250

[6] Hou Y. Vacuum-assisted resin infusion molding (VARIM) processing for thick-section composite laminates in wind turbine blades. In: Proceedings of the American Society for Composites 27th Technical Conference; 1–3 October 2012; Arlington. ASC Proceedings. 2012. pp. 334-351

[7] Li L. Interlaminar fatigue of thick-section glass fabric/vinyl ester composite [thesis]. Houston: University of Houston; 2013

[8] Makeev A, Nikishkov Y, Carpentier P, Lee E, Noel J. Manufacturing issues and measurement techniques for assessment of the effects on structural performance of composite parts. In: Proceedings of the American Helicopter Society 66th Annual Forum; 11–13 May 2010; Phoenix. 2010

[9] Griffin J. How to Dispose of 2-Part Epoxy Solutions [Internet]. 2013. Available from: https://www.lion.com/lion-news/april-2013/how-to-dispose-of-2-part-epoxy-solutions. [Accessed: October 16, 2019]

[10] Bailleul JL. Optimisation du cycle du caisson de pièces épaisses en matériau composite, Application a un préimprégné résine époxide/fibres de verre [thesis]. Nantes: Université de Nantes; 1997

[11] Nawab Y, Tardif X, Boyard N, Sobotka V, Casari P, Jacquemin F. Determination and modelling of the cure shrinkage of epoxy vinylester resin and associated composites by considering thermal gradients. Composites Science and Technology. 2012;**73**:81-87. DOI: 10.1016/j.compscitech.2012.09.018

[12] Hou Y, Wang SS. Analysis and Correlation of Curing Kinetics in Glass/Polyester Composite Processing by DSC and DEA Methods [Technical Report]. Houston: National Wind Energy Center; 2012

[13] Pascault JP, Sautereau H, Verdu J, Williams RJJ. Thermosetting Polymers. 1st ed. Boca Raton: CRC Press; 2002. 496 p. DOI: 10.1201/9780203908402

[14] Bailleul JL, Delaunay D, Jarny Y. Determination of temperature variable properties of composite materials: Methodology and experimental results. Journal of Reinforced Plastics and Composites. 1996;**15**:479-496. DOI: 10.1177/073168449601500503

[15] Buck W, Rudtsch S. Thermal properties. In: Czichos H, Saito T,

Smith L, editors. Springer Handbook of Materials Measurement Methods. Heidelberg: Springer Berlin Heidelberg; 2006. pp. 399-429. DOI: 10.1007/978-3-540-30300-8_8

[16] Li C, Potter K, Wisnom MR, Stringer G. In-situ measurement of chemical shrinkage of MY750 epoxy resin by a novel gravimetric method. Composites Science and Technology. 2004;**64**:55-64. DOI: 10.1016/S0266-3538(03)00199-4

[17] Shah DU, Schubel P. Evaluation of cure shrinkage measurement techniques for thermosetting resins. Polymer Testing. 2010;**29**:629-639. DOI: 10.1016/j.polymertesting.2010.05.001

[18] Khoun L, Hubert P. Cure shrinkage characterization of an epoxy resin system by two in situ measurement methods. Polymer Composites. 2010;**31**: 1603-1610. DOI: 10.1002/pc.20949

[19] White SR, Hahn HT. Process modeling of composite materials: Residual stress development during cure. Part II. Experimental validation. Journal of Composite Materials. 1992;**26**: 2423-2453. DOI: 10.1177/002199839202601605

[20] Bogetti TA, Gillespie JW Jr. Process-induced stress and deformation in thick-section thermoset composite laminates. Journal of Composite Materials. 1992;**26**: 626-660. DOI: 10.1177/002199839202600502